Chapter 1

Introduction and literature review

Chapter 1: Introduction and literature review

1.1. Introduction

Permanent magnets have today become inseparable components for several advanced devices. They are critical for a wide spectrum of applications ranging from motors to missiles. Several renewable energy systems like electric vehicle traction motors and wind turbine generators require permanent magnets. Hard magnets are also used in hard disk read heads, medical devices (MRI and NMR), magnetic MEMS, acoustics, bearings and several others. Further, the rapid strides in the advancements of the above discussed electromechanical conversion systems is largely owed to their miniaturization, which was made possible due to the improvements in the commercially available permanent magnets[1]. For instance, according to a comparative study for five horsepower applications, the space and weight reductions of nearly 70% and 60 % respectively was achieved when permanent magnet based motors were used instead of conventional induction motors [2]. Currently, the world permanent magnet market is estimated to be around 39 Billion USD. It is expected to reach 74 Billion USD by 2030 [3].

A typical permanent magnet is characterized by a considerable remanent magnetization even after the removal of the applied external magnetic field, denoted as M_r and a large resistance to demagnetization, referred to as coercivity (H_C). The temperature above which the ferromagnetic materials losses its magnetic ordering and transforms to a paramagnetic material is referred to as Curie temperature (T_C). However, the merit of a hard magnet is measured by its "energy product", $(BH)_{max,}$ which describes the strength of a magnet. It is pictorially represented in the second quadrant of the B-H Hysteresis curve as the area of the largest possible rectangle. The importance of the energy product for any hard

magnet lies in the fact that the volume of material required for any given application is inversely proportional to its energy product.

It is therefore justifiable to say that the saga of development of permanent magnetism terms of their energy product, helped in the compactness of modern devices. The Figure 1 shows the brief timeline of the evolution of the energy product of hard magnets beginning from the early 20^{th} century. Nevertheless, the first known permanent magnet around 4 B.C. to the humankind was naturally occurring "lodestone" or magnetite (Fe_3O_4) mineral, which was assumed to be magnetized by lightning strikes. This was used to magnetize steel compass needles in ancient civilizations [4]. Thus, compass needles are probably the foremost synthetic permanent magnets. However, even until the beginning of the 20^{th} century, the highest $(BH)_{max}$ achieved was only 1 MGOe and the strongest known magnets were prepared from martensitic carbon steels predominantly containing Fe, C, Cr and Co. In fact, the term "hard magnet" came into prevalence for permanent magnets because these steels are mechanically hard [5].

Gradually, in 1930's, further attempts to improve the energy product of these Fe based materials led to a new class of magnets called "Alnico", where Al, Ni and Co were added to Fe. The improvement in $(BH)_{max}$ was achieved due to its finely dispersed ferromagnetic (Fe and Co rich) needles in a non-ferromagnetic matrix (Al and Ni rich). This advancement caused the commercial replacement of electromagnets with Alnico for several applications. However, these magnets suffer "self-demagnetization" and can only be used in "horse-shoe" geometry [6]. Consequently, this shape limitation of Alnico's was overcome with the advent of "Hard-ferrites" in 1950's. Hard ferrites, hexagonal compounds of strontium and barium –

(e.g. $BaFe_{12}O_{19}$, $SrFe_{12}O_{19}$) are widely used today despite having a lower energy product than Alnico because of its shape flexibility, low cost, chemical stability and high corrosion resistance [7].

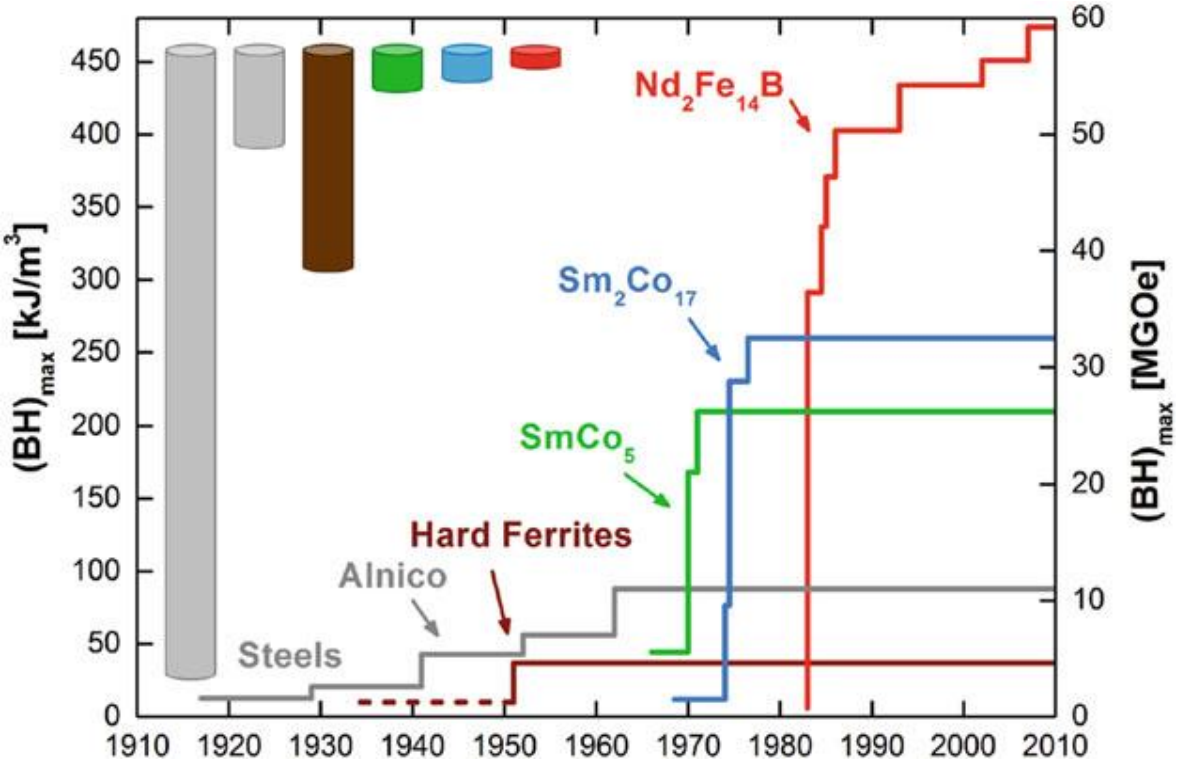

Figure 1.1. Historical development of energy product of permanent magnets in the 20th century. (Inset depicts the amount of material required for storage of the same magneto- static energy)[1].

The $(BH)_{max}$ improvement journey took a paradigm shift in the late 1960's and 1970's with the discovery of Sm-Co and Nd-Fe-B compounds respectively. $SmCo_5$ compound was first envisaged by K. J. Stratnt, G. Hoffer and others to utilize the combination of rare-earth elements with high magnetocrystalline anisotropy (K) and the 3d elements with large magnetization and high Curie temperatures [8]. The $SmCo_5$ based magnet was the first rare-earth based magnet. Further, Sm_2Co_{17} compound was also developed taking the maximum

energy product to nearly 30 MGOe and an operational temperature of up to 300 ºC [9]. Later in 1979, Sumitomo metals and General Motors simultaneously developed the $Nd_2Fe_{14}B$ tetragonal compound based magnets. By far, at room temperature, these are the strongest available magnets with the energy product almost reaching to 55 MGOe [10]. Thus, at present broadly four categories of magnets are available, the lower end Alnico and Ferrites and the two RE based magnets, Sm-Co and Nd-Fe-B magnets.

1.2. RE problem

Presently, Nd-based dominate around 50 % value of the permanent magnet market share. These rare-earth based magnets have an appreciable energy product at room temperature but their energy product falls drastically with rising temperature. Often, these magnets are required to operate at elevated temperatures like in the case of electric vehicle traction motors, where the localized temperature may rise up to 200 ºC. To slow down the rate of fall of Nd-based magnet with temperature, heavy rare-earth metals like Dysprosium (Dy) and Terbium (Tb) are added [11]. The challenge associated with rare-earth elements like Nd, Dy, Tb and Pr are that their natural occurrence and production are highly concentrated to a single country. In fact, the production of these RE-based magnets and RE oxides is also done predominantly by China (around 80% in 2018). In 2011, the restrictions laid on RE's by China led to the rare-earth crisis leading to a sharp rise in their prices (Figure 2). Nd, Dy and Tb have been marked as critical materials by US department of energy, NITI AYOG of India and other countries due to their supply chain risks and price concerns [12]. Sm-Co alloys are another type of rare-earth permanent magnets with better high temperature performance. However, the energy product of this material is lesser than that of Nd-Fe-B. Nonetheless, such alloys also have similar rare-earth (Sm) supply issues as well as Co price

concerns. This led to the quest for alternative magnetic materials for permanent magnet applications and reducing the rare-earth content by substitution, especially the heavy rare earths in Nd-based magnets. Apart from the geo-political factors, the challenges associated with this class of magnets can be broadly classified into four types: Technical, future demand, ecological and recycling potential.

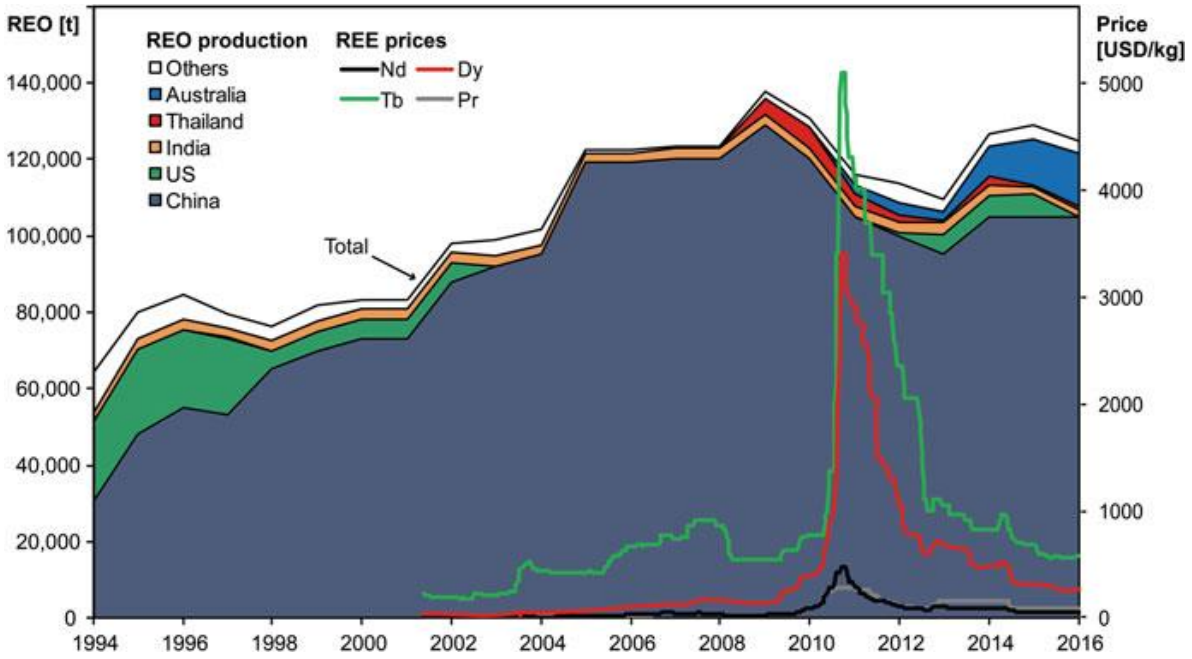

Figure 1.2. Rare-earth oxide production worldwide over the past few decades vs. Price movement of critical Nd, Dy, Tb and Pr metals[1].

Technical: There is an "energy product-gap" between the lower end ferrites and high-end Nd-based magnets. At present there is a need for an economic "Gap magnet" as termed by Coey et al. with an energy product greater than 5 MGOe and lower than 30 MGOe for several applications including elevated temperature scenarios. For such cases, currently, the relatively costlier and high-end RE magnets are used by dilution and reducing its energy product [13].

Future Demand: It is estimated that around wind turbines use around 600 kg of Nd-based magnets for 1 MW power production and a hybrid electric vehicle needs around 1 kg. According to 2015 statistics, around 150 kilo tonnes of Nd-Fe-B magnets alone were used annually [14]. As the world aims to reduce its CO_2 production and achieve net zero carbon emissions (NZE) by 2050, these alternate energy based technologies are bound to grow multi fold. However, such huge demand cannot be met by a single class of materials and require various materials for different applications.

Ecological and recycling potential: The RE-extraction process results hazardous radioactive substances, effluent acidic gases, liquid discharges and other mining wastes. In addition, the recycling of end-of-life magnets is also at a very nascent stage, with practically less than 1 percent of the total magnets produced being recycled [15]. Thus, the breakthrough of many new technologies, most notably robots, large-scale wind power applications, e-mobility, and energy-efficient industrial production equipment, will depend on overcoming these obstacles and developing alternate materials.

1.3. Rare-earth free permanent magnets

Despite the fact that the theoretically calculated energy product of the rare-earth free magnets are considerably lower than that of RE magnets, significant efforts are being carried out by the researchers to explore novel materials of less hazardous nature for a "Gap magnet". Several potential materials displaying high magnetocrystalline anisotropy (K_1) leading to good coercivity, high magnetization values along with a high Curie temperature and good chemical stability have piqued the interest of researchers and are tabulated below.

Table 1: Intrinsic properties of various RE free magnetic materials [16]

Compound	**Saturation magnetization**	**Curie Temperature (°C)**	**Anisotropy constant K_1 (MJ/m^3)**	**$(BH)_{max}$ MGOe**	**Merits/demerits**
Co (C)	17.6 kG	1115	0.53	78	Decomposes-500°C
FePt	14.3 kG	477	6.6	50	Expensive
CoPt	10.0 kG	567	4.9	25	Expensive
MnAl(C)	6.2 kG	377	1.7	10	Phase decomposition
MnBi	**8.5 kG**	**357**	**1.6**	**18**	**Phase change (340°C)**
Mn_2Ga	5.8 kG	500	2.3	9	Low Magnetization
$Fe_{16}N_2$	24 kG	537	1.0	144	Phase change(240°C)
Fe-C	13.6 kG	483	0.45	46	Phase decomposition
$L1_0$ FeNi	16 kG	500	0.32	64	Difficult to prepare
Alnico	14 kG	900	0.7	49	Shape Anisotropy
YCo_5	10.6 kG	714	6.5	26	Expensive
$BaFe_{12}O_{19}$	4.8 kG	450	0.33	6	Low energy product
Zr_2Co_{11}	≈10.2 kG	500	(H_A = 34 kOe)	25	Remanence

All the compounds are based on 3d- transition elements having non-cubic crystal structure. Each material system has merits and drawbacks in one or another property required for the development of permanent magnetic characteristics. Considering the cost and best

combination of anisotropy (K_1), magnetization and Curie temperature (T_c), LTP MnBi compound is a promising candidate for developing RE free permanent magnetic material amongst the RE free materials. Thus, the LTP MnBi material system has been selected in part of the work in this thesis.

1.4. Mn-Bi system

Manganese, among the ferromagnetic transition elements has the highest magnetic moment i.e. 3.6 μ_B per atom (Bohr Magneton) because of its highest number of valence electrons. Its large unit cell can accommodate Mn atoms at four different sites with μ_B/atom ranging from 0.5 to 3.6. Despite this, its exchange energy causes antiferromagnetic ordering in it according to the Bethe-Slater curve (figure 3), the antiferromagnetic coupling in Mn arises from its short interatomic distance. Generally, atoms on sites with the shortest Mn–Mn distances< 240 pm, tend to be diamagnetic, those in sites with distances in the range 250–280 pm have small itinerant moments, which tend to couple anti-ferromagnetically, and only manganese atoms in sites with the longest bonds, > 290 nm, tend to have larger moments, that couple ferromagnetically. If the interatomic spacing between Mn atoms is large enough, the exchange energy become positive and magnetic ordering can be achieved at room temperature. Alloying Mn with Al, Bi, or Ga gives the right spacing for the energy change and thus their alloys with specific compositions act as ferromagnetic. Out of various combinations, Mn-Bi, Mn-Al and Mn-Ga show hard magnetic properties [17].

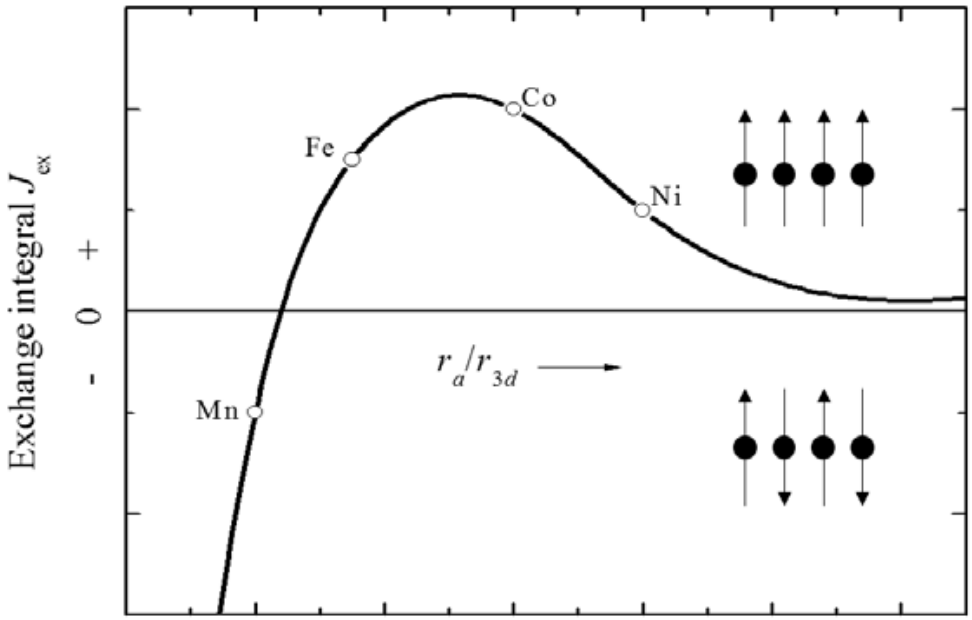

Figure 1.3. Schematic illustration of r_a /r_{3d} ratio versus exchange integral [18].

Out of these, the ferromagnetism in MnBi was first reported over a century ago. The ferromagnetic nature of manganese-bismuth alloys was first reported by Heusler about1904. This was confirmed by Arrivaut in 1905 and by others at about the same period. Guillaud thoroughly investigated this system and, in addition to measuring the saturation moment, magnetic crystal anisotropy, and Curie temperature, established experimentally the fact that the coercive force of the material increased with the reduction of particle size [19]. For an average particle diameter of 3.3 microns, he obtained an intrinsic coercive force on the loose powder of 12 kOe. He also concluded that a single phase, MnBi, was responsible for the ferromagnetic character of the alloy. The research on this system again gained momentum after the 2011 rare earth crisis. RE free Mn-based hard magnetic phases, especially the (LTP) MnBi has received considerable attention for a prospective “Gap Magnet” with energy product between the hard ferrites (5 MGOe) and RE magnets (30 MGOe).

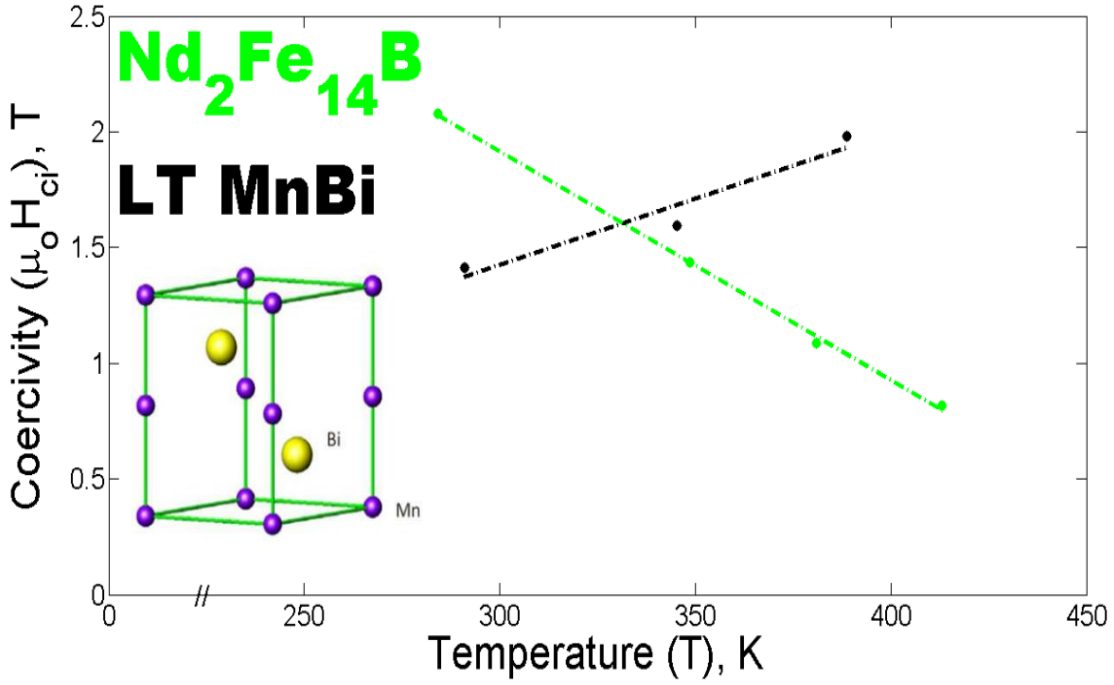

Figure 1.4. Temperature dependence of intrinsic coercivity of two ferromagnetic compounds (LTP MnBi and $Nd_2Fe_{14}B$). Inset depicts LTP MnBi hexagonal unit cell[20].

The theoretical saturation magnetization of Low Temperature Phase (LTP) MnBi is about 81 $emug^{-1}$ and the maximum theoretical energy product $(BH)_{max}$ is about 18 MGOe. However, the maximum energy product value obtained so far for bulk MnBi is around 8 MGOe [13]. Ferromagnetic intermetallic compound MnBi (crystal structure analogous to hexagonal NiAs, $B8_1$) possesses a large room temperature magnetocrystalline anisotropy of 1.6 MJm^{-3}. It exhibits a most intriguing feature of positive temperature coefficient of coercivity (H_C) i.e., intrinsic coercivity increases linearly with temperature. In fact, at 530 K, its H_C reaches 28.3 kOe, which is greater than that of Nd based RE Magnets at the same temperature (Figure 4). This unique feature of MnBi could prove favourable in high temperature applications where Nd based magnets show degrading properties.

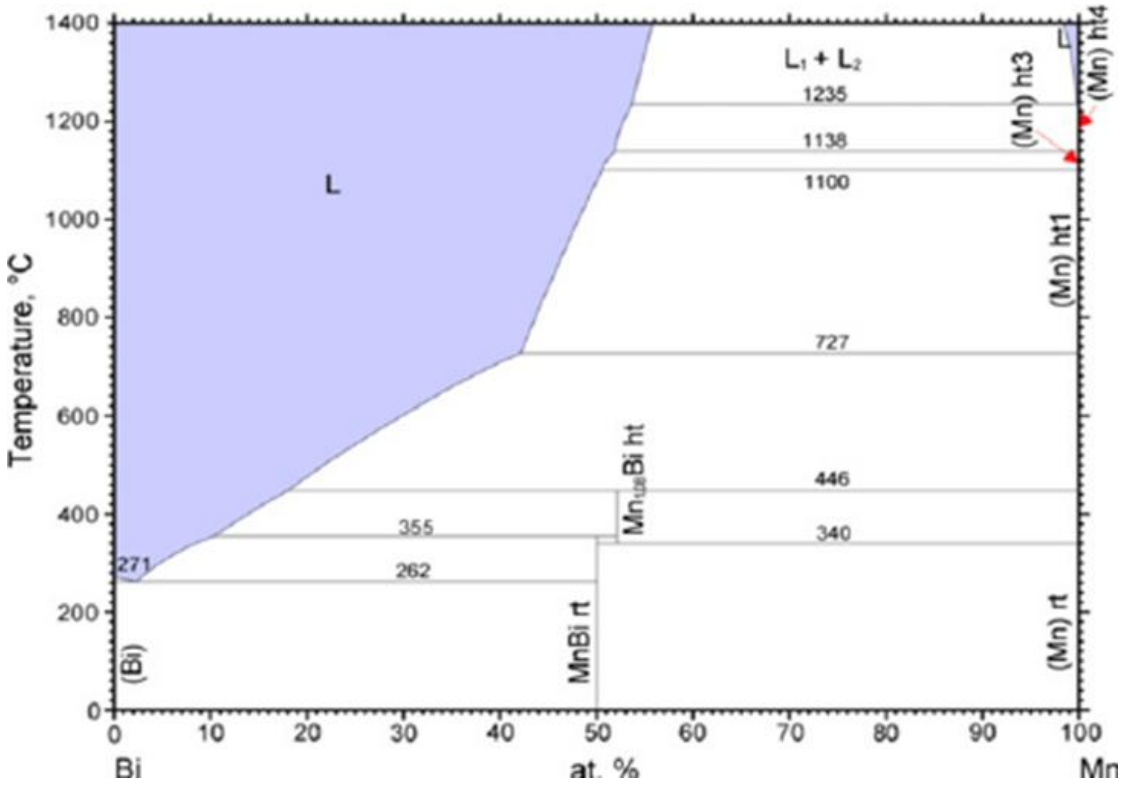

Figure 1.5. Mn-Bi phase diagram [21].

Though the first principle calculations indicate a high theoretical energy product $(BH)_{max}$ of 17.7 MGOe for LTP MnBi magnet, only 7.8 MGOe has been achieved till date in sintered bulk magnet at room temperature. This is due to the difficulty in preparing pure single-phase bulk LTP MnBi which forms as a result of a peritectic reaction (Figure 1.5). Nevertheless, LTP-MnBi based bulk magnet may be commercialized if its energy product exceeds 10 MGOe at room temperature in place of current value of 7.8 MGOe. Further, the raw materials cost of MnBi is less than $15/kg as of January 2018.

Several approaches have been employed to prepare MnBi over the past decades including arc melting [22], rapid solidification [23], mechanical alloying [24] and sintering [25]. For example, Guo et al. [26] reported obtaining single-phase LTP MnBi over 95 wt.%

by rapid quenching from melt to room temperature followed by thermal annealing but the coercivity was only 2 kOe at room temperature. Yoshida et al. [22] produced LTP MnBi of about 90 wt.% of the single phase by zone-arc-melting under a He atmosphere. Ko et al. [26] fabricated MnBi magnets with coercivity value of 10 kOe and $(BH)_{max}$ up to 5.34MGOe using mechanically alloyed powders via the spark plasma-sintering process. Recently, Yang et al. [27] reported over 90 wt. % LTP MnBi bulk samples produced by sintering and subsequent magnetic purification. The $(BH)_{max}$ up to 7.7 and 4.6 MGOe was achieved at 300 and 400 K, respectively.

The H_C of a magnet is microstructure sensitive and largely gets influenced by particle size. The optimum H_C is expected when the particle size equals to the critical diameter for single domains (D_C). This is referred to as the "size effect" and is shown in Figure 6. In 1950, Guillaud, Kondo, and Thielman [19, 28] investigated H_C of poorly compacted MnBi magnets and observed that H_C of these magnets can be improved by refining the particle size. Therefore, particle refinement is a potential approach to improve H_C of LTP MnBi magnets.

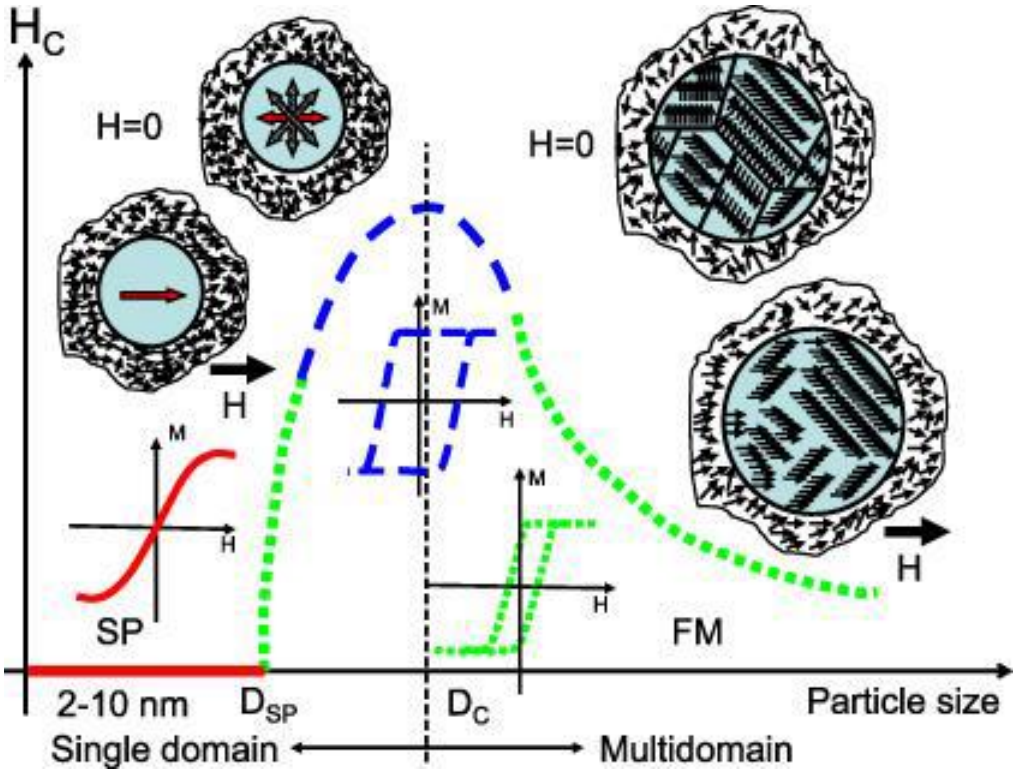

Figure 1.6. The variation of coercivity and saturation magnetization as a function of particle size [29].

However, the inherent low remanent magnetization value is one of the prominent reasons for the deviation of practical energy product from the calculated one. This also arises fundamentally from the "Manganese Dilemma", to obtain a large moment, the manganese atoms have to be fairly well separated, which naturally reduces the magnetization because M_S is the magnetic moment per unit volume. To overcome this challenge, exchange-coupled nanocomposite magnets can be prepared using LTP MnBi as the hard phase with soft magnetic phases. Composite LTP MnBi/$Nd_2Fe_{14}B$ [30] and LTP MnBi/Bi [31] magnets have been reported at the nanoscale, however, they are not considered as true nanocomposites because both $Nd_2Fe_{14}B$ and LTP MnBi are hard magnets, and -Bi is diamagnetic.

Therefore, neither $Nd_2Fe_{14}B$ nor Bi fulfills the definition of an exchange-coupled magnet, i.e. a combination of hard and soft magnetic phases at the nano-regime.

1.5. Exchange-coupled magnets

Different from what we have seen in the last century, the new generations of permanent magnets may not be based on single-phase magnetic alloys and compounds but composite materials of known hard and soft magnetic phases with required nanoscale morphology. In such composites, the soft phase provides the high magnetization and the hard phase provides the magnetic anisotropy. Several groups are working to push the energy density to the theoretical value or higher by adding soft magnetic phases to form a nanocomposite magnet.

For example, in 1989, Coehoorn et al. [32] first observed remanence enhancement in isotropic $Nd_2Fe_{14}B/Fe_3B$ composite magnets and ascribed it to intergrain exchange coupling. In 1991, Kneller and Hawig [33] proposed their simulation model to obtain high-energy product by making an exchange-coupled hard/soft nanocomposite magnet, also referred to as exchange-spring magnets. The concept was further explored by Skomski and Coey [34] theoretically and a prediction was given that a giant energy product of 120 MGOe can be attainable in an oriented nanostructured $Sm_2Fe_{17}N_3$/FeCo composite magnet.

Soft ferromagnets usually have very low H_C but often exhibit high magnetization. Ferromagnetic metals like Fe or Co are known soft magnets. Usually the ferromagnetic domains in soft magnets follow nucleation motion without any pinning which causes the spins to be rotated easily with the applied magnetic field. $Fe_{65}Co_{35}$ is an alloy soft magnet which has the highest magnetization among all known materials with J_S value of about 25

kG and often used as the soft phase in a composite magnet. The critical length of the soft phase required for perfect exchange coupling between hard and soft phases is less than about twice the length of Bloch wall width [35].

$$\delta h = \sqrt{A/K_h} .$$

A Bloch wall (δh) is defined as the region where the magnetization changes its value from one domain to the other and A and K_h are the exchange-stiffness constant and magnetic anisotropy constant of the hard phase respectively.

Usually, the critical length discussed above is within the nanoscale region and producing perfectly exchange coupled magnets in bulk form are not easy. The soft magnetic phase (m) controls the average exchange energy resulting in high B_r whilst the hard magnetic phase (k) governs the magnetic anisotropy of the magnets leading to a high H_C. The magnet overcomes the traditional inverse relationship between B_r and H_C by the exchange coupling effect between m and k [33].

The coupling effect allows the two magnetic phases to interact as though they are a single magnetic phase and therefore combines the advantages of both m and k in permanent magnets. Figure 1.7 illustrates the ‘spring mechanism’ [33] when a magnetized material undergoes demagnetization.

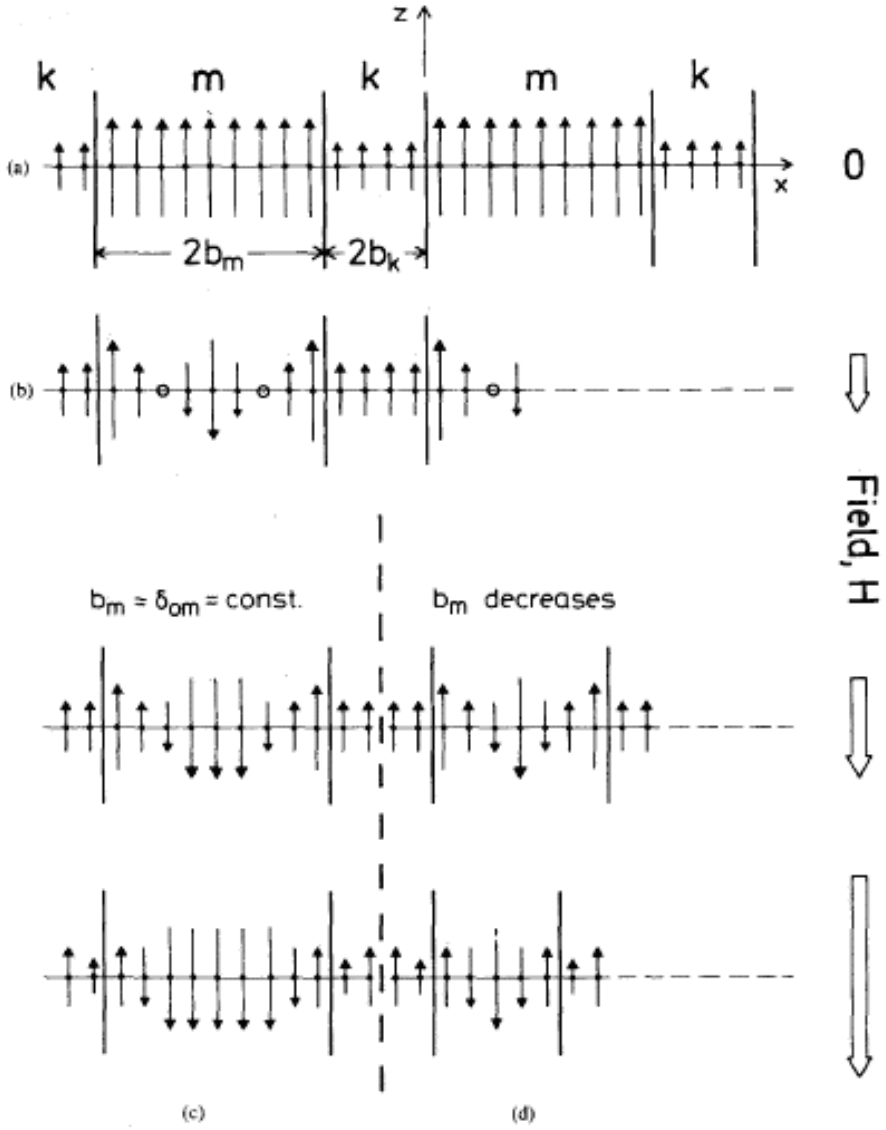

Figure 1.7. Schematic of one-dimensional model of the exchange coupled composite material. Direction "z" indicates the field, applied in the easy direction, (a) saturation remanence, (b)-(c) demagnetization in an increasing reverse field H, and (d) demagnetization [33].

The figure shows the arrangement of m and k next to one another in an alternating manner. As the material demagnetizes from J_s, m_s at the centre of m will begin to rotate while

the moments at the boundaries near k remain unaffected. This is because the anisotropy constant for m is lower than k. Consequently, two 180° equilibrium walls are formed. At higher field, the energy of these walls increases resulting in an increase in energy density of the wall above the equilibrium energy density of m. This process will continue until it approaches the equilibrium energy density of k. At this energy state, the moment at the boundary of m near k can rotate the moment of k. This phenomenon gives rise to the magnetization reversal of the magnetic phases and explains B_r and H_C enhancement as the particle size approaches nanoscale [30].

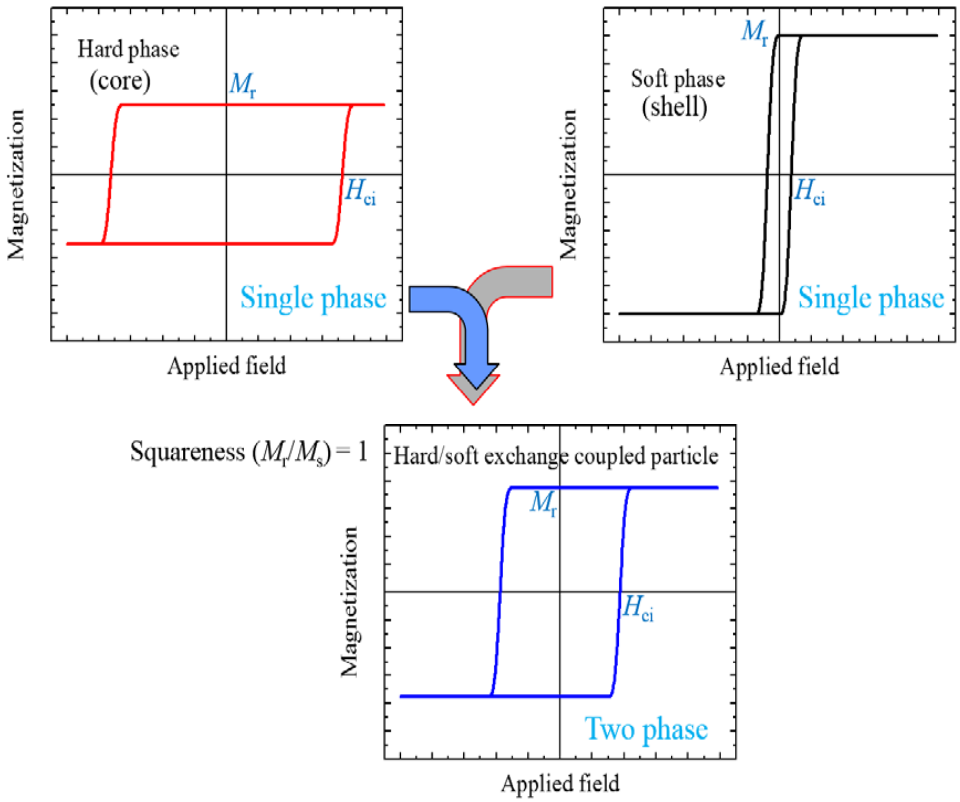

Figure 1.8. M vs H loops of hard, soft and exchange coupled materials [18].

Micro-magnetic simulation studies predicted the possibility of an energy product, as high as 40 MGOe, in case of perfect ferromagnetic exchange interaction between MnBi and

α-Fe nanocomposite system [37]. Similarly, energy products of around 25 MGOe were predicted in simulation studies for MnBi/Co and MnBi/$Fe_{65}Co_{35}$ magnets respectively [38]. Experimentally, Gao et al. reported an energy product of 25 MGOe for the exchange coupled thin films of MnBi and FeCo [39]. Exchange coupling in MnBi/FeCo nanowires and MnBi/FeCo core-shell structures have also been attempted but the energy product remained below 6 MGOe [40]. In other hard magnetic systems like Sm-Co and Nd-Fe-B, previous reports often employed α-Fe or $Fe_{65}Co_{35}$ as the soft magnetic phases when creating exchange spring magnets [41-43]. Table 2 shows crucial magnetic properties of these phases. However, these soft phases are prone to oxidation, which negatively affects the overall physical properties including magnetic behaviors.

Table 2. Magnetic properties of commonly used soft-phases in exchange-spring magnets

Phase	**M_S (T)**	**K_1 (kJ/m^3)**	**T_C (°C)**
$Fe_{65}Co_{35}$	2.45	20	937
α-Fe	2.15	48	771
Co	1.8	410	1087

The concept of exchange-coupled nanocomposite magnets provides an excellent opportunity for materials design for permanent magnets for future applications. It is feasible to design and devise a composite permanent magnet that has all the required properties by choosing suitable hard and soft phases and by adjusting their ratio. In the meantime, the materials cost of the composite magnets should be significantly lower than the single-phase hard magnetic materials because the soft phases (transition metal based) are always cheaper.

High-energy ball milling can be an efficient method for preparing such nanocomposites, and has been adopted by many groups in the fabrication of such magnet systems [42].

1.6. Motivation

Preparation of single phase MnBi, which forms through peritectic reaction at a relatively low temperature, is difficult by conventional synthesis techniques such as arc-melting, rapid solidification and sintering. In this work, we propose the fabrication of anisotropic MnBi magnet with superior $(BH)_{max}$ by adopting a combination of high-energy cryogenic ball milling (HECBM) and exchange coupling with a soft phase. MnBi bulk magnets were made using mechanically milled powders, resulting in coercivity values of approximately 10 kOe and an energy product of about 5.3 MGOe [44,45]. However, ball milling for more than 2 h at room temperature causes the desired low temperature phase to dissociate. This decomposition increases the presence of a secondary phases (Mn and Bi), which is non-ferromagnetic and malleable. Consequently, due to Bi phase, reduction of the size of the low temperature phase becomes challenging. Consequently, overall magnetization decreases with increased milling duration [46]. To address this issue of phase breakdown during ball milling, cryo-milling has been adopted in the present work. This technique reduces the overall milling time required to achieve similar particle size reduction. Additionally, the cryogenic temperature slows down the occurrence of phase breakdown and possible oxidation that may happen during milling at room temperature.

After the formation of MnBi phase, its nanocomposites were prepared using various proportions of carbon coated soft ferromagnetic nanoparticles (Co@C, Fe_3C@C and @FeNi@C) by the combination of above techniques. Previous studies have explored Co, FeNi and Fe_3C as soft phases for exchange coupled magnets but in this study carbon coated

soft phases were envisaged to prevent oxidation and also utilize the benefit of carbon interaction with MnBi. Hexagonal Co, Cubic FeNi and orthorhombic Fe_3C nanoparticles, all have a high saturation magnetization and low coercivity making them probable candidates for the soft phase.

The obtained powders at various stages were characterized by X-ray diffraction (XRD), scanning electron microscopy (SEM) equipped with energy dispersive X-ray spectroscopy (EDX), high-resolution transmission electron microscopy (HRTEM), x-ray photoelectron spectroscopy (XPS), raman spectroscopy and magnetic properties measurement system (MPMS).

1.7. Objectives:

1. Preparation of MnBi based REFPMs by vacuum arc-melting followed by comparative studies of its room temperature and cryogenic ball milling.
2. Preparation of nanocomposites of MnBi with various proportions of magnetic nanoparticles (e.g. Co@C, Fe_3C@C and FeNi@C) by previously mentioned techniques.
3. Structural, microstructural and magnetic properties evaluation of Mn-Bi alloys and its nanocomposites to decipher the underlying phenomena affecting the magnetic properties.

1.8. References

[1] O. Gutfleisch, M.A. Willard, J.P. Liu, Magnetic materials and devices for the 21st century: Stronger, lighter, and more energy efficient, Adv. Mater. 23 (2011) 821–842.

[2] J. Kang, General purpose permanent magnet motor drive without speed and position sensor, Yaskawa Electr. Am. 27 (2009) 1005–1011.

[3] J.W. Heim, R.L. Vander Wal, NdFeB Permanent Magnet Uses, Projected Growth Rates and Nd Plus Dy Demands across End-Use Sectors through 2050: A Review, Minerals. 13 (2023) 1274.

[4] M. Schlenker, Magnetism: Materials and applications, Springer Verlag, 2005.

[5] J.D. Livingston, Driving Force: The natural magic of magnets, (No Title). (1996).

[6] R.A. McCurrie, The structure and properties of alnico permanent magnet alloys, Handb. Ferromagn. Mater. 3 (1982) 107–188.

[7] J.J. Went, G.W. Rathenau, E.W. Gorter, G.W. van van Oosterhout, Hexagonal iron-oxide compounds as permanent-magnet materials, Phys. Rev. 86 (1952) 424.

[8] K. Strnat, G. Hoffer, J. Olson, W. Ostertag, J.J. Becker, A family of new cobalt-base permanent magnet materials, J. Appl. Phys. 38 (1967) 1001–1002.

[9] K.J. Strnat, R.M.W. Strnat, Rare earth-cobalt permanent magnets, J. Magn. Magn. Mater. 100 (1991) 38–56.

[10] D. Harimoto, Y. Matsura, Development of ultra-high quality NdFeB permanent magnet, Hitachi Met, Tech. Rev. 23 (2007) 69–72.

[11] S. Sugimoto, Current status and recent topics of rare-earth permanent magnets, J.

Phys. D. Appl. Phys. 44 (2011). https://doi.org/10.1088/0022-3727/44/6/064001.

[12] J. Cui, M. Kramer, B. Balasubramanian, D. Sellmyer, Current progress and future challenges in rare-earth-free permanent magnets, Acta Mater. 158 (2018) 118–137.

[13] J.M.D. Coey, Permanent magnets: Plugging the gap, Scr. Mater. 67 (2012) 524–529.

[14] K.-H. Müller, S. Sawatzki, R. Gauß, O. Gutfleisch, Permanent magnet materials and applications, in: Handb. Magn. Magn. Mater., Springer, 2021: pp. 1369–1433.

[15] X.-Y. Li, J.-P. Ge, W.-Q. Chen, P. Wang, Scenarios of rare earth elements demand driven by automotive electrification in China: 2018–2030, Resour. Conserv. Recycl. 145 (2019) 322–331. https://doi.org/10.1016/j.resconrec.2019.02.003.

[16] M.J. Lucis, Microstructure and phase analysis in Mn-Al and Zr-Co permanent magnets, The University of Nebraska-Lincoln, 2015.

[17] J. Yang, W. Yang, Z. Shao, D. Liang, H. Zhao, Y. Xia, Y. Yang, Mn-based permanent magnets, Chinese Phys. B. 27 (2018).

[18] J. Park, Rare-earth free permanent magnets and permanent magnet synchronous motors, (2016).

[19] C. Guillaud, Polymorphisme du composé défini Mn Bi aux températures de disparition et de réapparition de l'aimantation spontanée, J. Phys. Radium. 12 (1951) 143.

[20] J.B. Yang, W.B. Yelon, W.J. James, Q. Cai, S. Roy, N. Ali, Structure and magnetic properties of the MnBi low temperature phase, J. Appl. Phys. 91 (2002) 7866–7868.

[21] H. Okamoto, H. Okamoto, Phase diagrams for binary alloys, ASM international Materials Park, OH, 2000.

[22] H. Yoshida, T. Shima, T. Takahashi, H. Fujimori, Preparation of highly pure MnBi intermetallic compounds by arc-melting, Mater. Trans. JIM. 40 (1999) 455–458.

[23] X. Guo, X. Chen, Z. Altounian, J.O. Ström-Olsen, Magnetic properties of MnBi prepared by rapid solidification, Phys. Rev. B. 46 (1992) 14578.

[24] W. Xie, E. Polikarpov, J.P. Choi, M.E. Bowden, K. Sun, J. Cui, Effect of ball milling and heat treatment process on MnBi powders magnetic properties, J. Alloys Compd. 680 (2016) 1–5. https://doi.org/10.1016/J.JALLCOM.2016.04.097.

[25] F. Yin, N. Gu, T. Shigematsu, N. Nakanishi, Sintering formation of low temperature phase MnBi and its disordering in mechanical milling, J. Mater. Sci. Technol. 12 (1996) 335–341.

[26] K.Y. Ko, S.J. Choi, S.K. Yoon, Y.S. Kwon, MnBi magnets fabricated through spark plasma-sintering process, J. Magn. Magn. Mater. 310 (2007) e887–e889.

[27] J.B. Yang, K. Kamaraju, W.B. Yelon, W.J. James, Q. Cai, A. Bollero, Magnetic properties of the MnBi intermetallic compound, Appl. Phys. Lett. 79 (2001) 1846–1848.

[28] K. Thielmann, Der Ferromagnetismus und sein Träger im System Mangan-Wismut, Ann. Phys. 429 (1940) 41–62.

[29] N. Paunović, Z. V Popović, Z.D. Dohčević-Mitrović, Superparamagnetism in iron-doped CeO2− y nanocrystals, J. Phys. Condens. Matter. 24 (2012) 456001.

[30] V. Ly, Nanostructural formation and magnetic properties of Fe-B-Nd and Mn-Bi permanent magnets, (2014).

[31] Y. Liu, J. Zhang, S. Cao, X. Zhang, G. Jia, Z. Ren, X. Li, C. Jing, K. Deng, Microstructure, crystallization, and magnetization behaviors in MnBi− Bi composites aligned by applied magnetic field, Phys. Rev. B. 72 (2005) 214410.

[32] R. Coehoorn, R.A. De Groot, The electronic structure of MnBi, J. Phys. F Met. Phys. 15 (1985) 2135.

[33] E.F. Kneller, R. Hawig, The exchange-spring magnet: a new material principle for permanent magnets, IEEE Trans. Magn. 27 (1991) 3560–3588.

[34] R. Skomski, J.M.D. Coey, Giant energy product in nanostructured two-phase magnets, Phys. Rev. B. 48 (1993) 15812–15816. https://doi.org/10.1103/PhysRevB.48.15812.

[35] R. Gao, W. Feng, W. Chen, B. Wang, G. Han, P. Zhang, Exchange-coupling interaction and effective anisotropy in nanocomposite permanent materials, Chinese Sci. Bull. 47 (2002) 1166–1169.

[36] G. Herzer, Anisotropies in soft magnetic nanocrystalline alloys, J. Magn. Magn. Mater. 294 (2005) 99–106.

[37] Y.Q. Li, M. Yue, J.H. Zuo, D.T. Zhang, W.Q. Liu, J.X. Zhang, Z.H. Guo, W. Li, Investigation of Magnetic Properties of MnBi/alpha-Fe Nanocomposite Permanent Magnets by Micro-Magnetic Simulation, IEEE Trans. Magn. 49 (2013) 3391–3393.

[38] J.P. Perdew, J.A. Chevary, S.H. Vosko, K.A. Jackson, M.R. Pederson, D.J. Singh, C. Fiolhais, Atoms, molecules, solids, and surfaces: Applications of the generalized gradient approximation for exchange and correlation, Phys. Rev. B. 46 (1992) 6671.

[39] X. Xu, Y.-K. Hong, J. Park, W. Lee, A.M. Lane, J. Cui, Magnetic self-assembly for

the synthesis of magnetically exchange coupled MnBi/Fe–Co composites, J. Solid State Chem. 231 (2015) 108–113.

[40] S. Li, L. Ma, J. Fan, J. Yang, Q. Zheng, B. Bian, J. Zhang, J. Du, High energy product of isotropic bulk Sm-Co/α-Fe (Co) nanocomposite magnet with multiple hard phases and nanoscale grains, J. Mater. Sci. Technol. 88 (2021) 183–188.

[41] L. Ma, W. Quan, J. Fan, Y. Chen, Q. Zheng, B. Bian, J. Zhang, J. Du, High magnetic energy product in isotropic nanocomposite powders with high percent of soft phase towards ultrastrong magnets, J. Mater. Sci. Technol. 144 (2023) 161–167.

[42] J. You, Q. Meng, J. Zhou, Y. Guo, Magnetic properties and air stability of BaFe12O19/Fe5C2 composites fabricated through cryogenic ball milling, Ceram. Int. 45 (2019) 15730–15735. https://doi.org/10.1016/J.CERAMINT.2019.05.009.

[43] C. Rong, Y. Zhang, N. Poudyal, I. Szlufarska, R.J. Hebert, M.J. Kramer, J.P. Liu, Self-nanoscaling of the soft magnetic phase in bulk SmCo/Fe nanocomposite magnets, J. Mater. Sci. 46 (2011) 6065–6074.

[44] D.T. Zhang, S. Cao, M. Yue, W.Q. Liu, J.X. Zhang, Y. Qiang, Structural and magnetic properties of bulk MnBi permanent magnets, J. Appl. Phys. 109 (2011) 07A722.

[45] E. Adams, A new permanent magnet from powdered manganese bismuthide, Rev. Mod. Phys. 25 (1953) 306.

[46] W. Xie, E. Polikarpov, J.-P. Choi, M.E. Bowden, K. Sun, J. Cui, Effect of ball milling and heat treatment process on MnBi powders magnetic properties, J. Alloys Compd. 680 (2016) 1–5.